Research Article | Vol. 29, No. 10 / 10 May 2021 / Optics Express 14345
Optics EXPRESS

Non-Hermitian effective medium theory and complex Dirac-like cones

LIYOU LUO,[1,4] YUMING SHAO,[1,4] JENSEN LI,[2] RENHAO FAN,[1] RUWEN PENG,[1] MU WANG,[1] JIE LUO,[3,5] AND YUN LAI[1,6]

[1]MOE Key Laboratory of Modern Acoustics, National Laboratory of Solid State Microstructures, School of Physics, and Collaborative Innovation Center of Advanced Microstructures, Nanjing University, Nanjing 210093, China
[2]Department of Physics, The Hong Kong University of Science and Technology, Clear Water Bay, Hong Kong, China
[3]School of Physical Science and Technology, Soochow University, Suzhou 215006, China
[4]These authors contributed equally
[5]luojie@suda.edu.cn
[6]laiyun@nju.edu.cn

Abstract: In this work, we propose a non-Hermitian effective medium theory to interpret the spawning rings of exceptional points out of the Dirac cones in the band structures of photonic crystals with loss/gain. Based on this theory, we predict and demonstrate two unique types of band dispersions of fully passive photonic crystals. In one type, the exceptional ring shrinks into a complex Dirac point associated with a complex Dirac-like cone. In the other type, a point of quadratic degeneracy is realized in the imaginary frequency spectrum. Our theory provides a unified picture for the exceptional points in effective media and gives rise to novel concepts like complex Dirac-like cones in non-Hermitian photonics.

1. Introduction

The effective medium theory [1,2] has provided a powerful tool in the fields of metamaterials [3] and photonic crystals (PhCs) [4] to explain the band dispersions at low frequencies. It has been discovered that when the effective permittivity and permeability accidentally cross zero at the same frequency, a Dirac point would appear at the Brillouin zone center with conical dispersions in its vicinity [5]. Moreover, there are simultaneously flat bands crossing the Dirac point, which coincide well with the mathematical condition of the longitudinal electromagnetic modes, i.e. zero permittivity or permeability component. Therefore, the effective medium theory can perfectly explain both the Dirac conical dispersion as well as the associated flat bands of longitudinal modes. Such unique dispersions and effective parameters have been observed in various frequency regime of electromagnetic and acoustic waves [5–16] and may have many important applications such as photonic chips [8–10], cloaking [11] and coherent perfect absorption [12,13], etc.

Recently, by introducing loss into the PhC with Dirac-like conical dispersion (Dirac cones plus the flat bands of longitudinal modes), the emergence of the spawning rings of exceptional points (EPs) out of the Dirac cones has been observed [17–21]. Inside the ring of EPs, the real parts of the eigen-frequencies have degenerate flat dispersions, while the imaginary parts split into two branches. Outside the ring of EPs, the situations are just the opposite. The real parts split, while the imaginary parts tend to degeneracy. Additional flat bands of longitudinal modes also emerge in the band structure of such non-Hermitian PhCs, but was not incorporated into the Hamiltonian model. Very recently, extensive efforts have been made to establish an effective medium theory for the non-Hermitian PhCs [22–24]. However, so far, a neat explanation of the ring of EPs from the effective medium point of view is still lacking.

#425862 https://doi.org/10.1364/OE.425862
Journal © 2021 Received 23 Mar 2021; revised 21 Apr 2021; accepted 21 Apr 2021; published 26 Apr 2021

Optics EXPRESS

In this work, we extend the local effective medium theory [5] to the non-Hermitian regime. In this picture, we assume that the effective parameters are independent of the wave vector, but dependent on both the real and imaginary parts of the angular frequency, i.e. $\omega = \omega_R + i\omega_I$. Here, ω_R describes the oscillating frequency, and ω_I describes the decaying or amplifying rate of waves. Recently, it has been demonstrated that ω_I can introduce the role of "effective gain" or "effective loss", which can be conveniently controlled by increasing or decreasing the intensity of incident waves at a certain rate [25,26]. Here, by extending the frequency dispersion from ω_R to ω_I, we have established a simple local effective medium which can not only explain the rings of EPs but also predict the occurrence and position of the additional flat bands in the band structure. Based on this picture, we further show two other unique types of band dispersions. One type has Dirac-like cones in both the ω_R and ω_I band structures, and the other type has a band gap and a point of quadratic degeneracy in the ω_R and ω_I band structures, respectively. Both dispersions have been verified by designing non-Hermitian PhCs. Our work paves a road for the manipulation of EPs and Dirac cones in the framework of non-Hermitian effective medium.

We start from the Hermitian PhC model (i.e. without loss or gain) with accidental Dirac-like cone occurring at the Brillouin zone center [5]. The PhC can be characterized by effective permittivity $\varepsilon(\omega)$ and permeability $\mu(\omega)$ as a linear function of frequency:

$$\begin{cases} \varepsilon(\omega) = A_\varepsilon \times (\omega - \omega_\varepsilon), \\ \mu(\omega) = A_\mu \times (\omega - \omega_\mu), \end{cases} \tag{1}$$

where $\omega_\varepsilon = \omega_\mu = \omega_D$, and A_ε and A_μ are approximately real constants in the small frequency regimes near ω_ε and ω_μ. As demonstrated previously, the degeneracy of zero permittivity and permeability at the same frequency ω_D would lead to the formation of Dirac cones with ω_D as the Dirac point frequency [17–21]. Near the Dirac point, ω varies almost linearly with the wave vector $\mathbf{k}$.

Equation (1) holds for the Hermitian system without loss or gain. When loss/gain is introduced into the system, the eigen-frequency turns into a complex one as $\omega = \omega_R + i\omega_I$. Here we consider the time variation term $e^{-i\omega t}$ such that $\omega_I > 0$ (or $\omega_I < 0$) indicates the amplification (or attenuation) of electromagnetic wave energy. Generally, the effective permittivity $\varepsilon(\omega)$ and permittivity $\mu(\omega)$ are complex and dispersive, which can be expressed as $\varepsilon(\omega) = \varepsilon_R(\omega) + i\varepsilon_I(\omega)$ and $\mu(\omega) = \mu_R(\omega) + i\mu_I(\omega)$. In a small frequency regime near the Γ point, we propose the following linear relation between the effective parameters and the eigen-frequency in a similar form of Eq. (1) with complex A_ε and A_μ:

$$\begin{cases} \varepsilon_R(\omega_R) = A_{\varepsilon_R} \times (\omega_R - \omega_{\varepsilon_R}), \\ \mu_R(\omega_R) = A_{\mu_R} \times (\omega_R - \omega_{\mu_R}), \\ \varepsilon_I(\omega_I) = A_{\varepsilon_I} \times (\omega_I - \omega_{\varepsilon_I}), \\ \mu_I(\omega_I) = A_{\mu_I} \times (\omega_I - \omega_{\mu_I}), \end{cases} \tag{2}$$

where the coefficients $A_{\varepsilon_R}, A_{\mu_R}, A_{\varepsilon_I}$ and A_{μ_I} satisfy $A_{\varepsilon_R} \approx A_{\varepsilon_I} \approx A_\varepsilon$ and $A_{\mu_R} \approx A_{\mu_I} \approx A_\mu$, in order to have complex Dirac-like cones. With the introduction of the loss/gain into the system, the effective medium turns into a non-Hermitian one, whose dispersion is changed by the loss/gain. When the loss/gain is relatively small, ω_{ε_R} and ω_{μ_R} are close to the ω_D, which is the Dirac point frequency in absence of loss/gain. In the complex frequency space, the dispersion relation can be expressed as,

$$(\omega_R + i\omega_I)^2(\varepsilon_R + i\varepsilon_I)(\mu_R + i\mu_I) = c^2\mathbf{k}^2, \tag{3}$$

where $\mathbf{k}$ is the in-plane wave vector (k_x, k_y), and c is the speed of light in free space. Equation (3) is a general dispersion relation, and is applicable for both Hermitian and non-Hermitian models.

Optics EXPRESS

In order to verify the validity of Eq. (2), we demonstrate a practical case of PhC by using the finite-element software COMSOL Multiphysics. First, we construct a Hermitian PhC with a Dirac-like cone. The PhC is composed of a square array of dielectric cylindrical rods in free space. The unit cell is illustrated by the inset graph in Fig. 1(a). The lattice constant is a. The radius and relative permittivity of the dielectric cylindrical rods are $R_a = 0.2a$ and $\varepsilon_A = 12.5$, respectively. For transverse-magnetic (TM, electric field along the rods) modes, such a PhC has a Dirac-like cone with Dirac point frequency $\omega_D a/2\pi c = 0.541$, due to the accidental degeneracy of the monopole mode and the degenerate dipole modes at the Γ point [5]. Then, we assume that the ε_A is changed to be complex as $\varepsilon_A = 12.5 + 0.5i$ in the frequency regime of interest. The positive imaginary part indicates loss in the rods and turns the PhC into a non-Hermitian system. The band structures in terms of ω_R and ω_I are shown in Figs. 1(a) and 1(b), respectively. They are calculated along the Γ − X direction. It is seen that the Dirac-like conical dispersion evolves into the interesting phenomenon of a spawning ring of EPs [17].

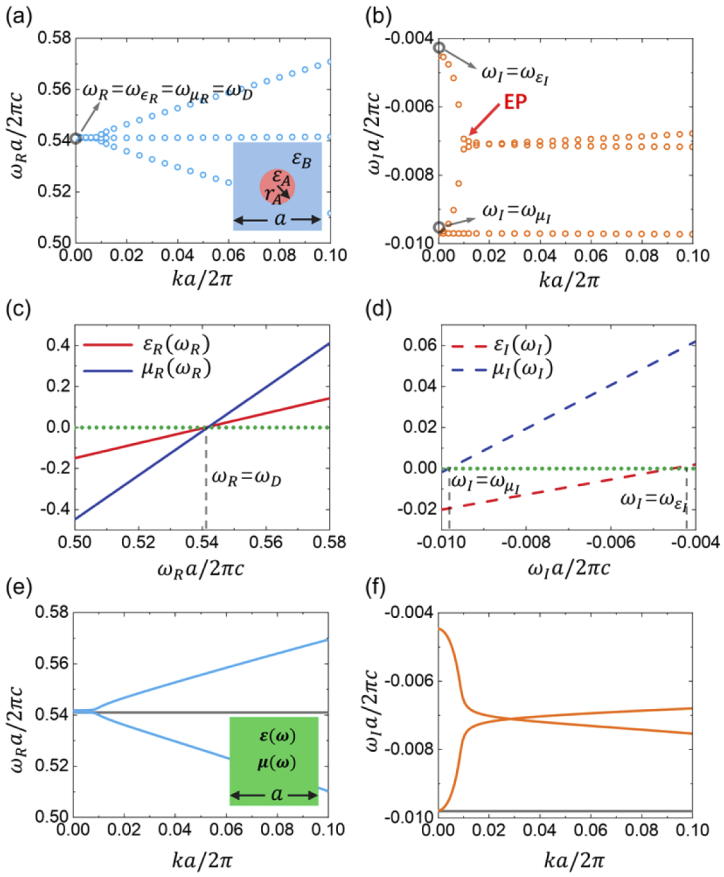

Fig. 1. [(a) and (b)] Complex band structures of a PhC composed of cylindrical rod with $\varepsilon_A = 12.5 + 0.5i$ in background medium of $\varepsilon_B = 1$. (a) and (b), respectively, show the real and imaginary parts of eigen-frequencies for given real Bloch wave vectors based on numerical calculations. (c) Real and (d) imaginary parts of the effective parameters of this PhC. Retrieved (e) real and (f) imaginary parts of eigen-frequencies based on the effective parameters. The gray solid line denotes the longitudinal mode.

Optics EXPRESS

This emergence of the ring of EPs is usually understood within a k.p approximation by constructing the effective Hamiltonian $H_{eff} = \begin{pmatrix} \omega_D & v_g|\mathbf{k}| \\ v_g|\mathbf{k}| & \omega_D - i\gamma_d \end{pmatrix}$ with complex eigen-frequencies as [17],

$$\omega = \omega_D - i\frac{\gamma_d}{2} \pm v_g\sqrt{|\mathbf{k}|^2 - k_c^2}, \tag{4}$$

where ω_D and v_g are angular frequency and group velocity of the linear Dirac dispersion in absence of loss/gain, respectively. The quantity γ_d describes the gain and loss, and $k_c \equiv \gamma_d/2v_g$. When $\gamma_d = 0$, Eq. (4) is simplified to $\omega = \omega_D \pm v_g|\mathbf{k}|$, which describes the formation of the Dirac-like cone in the Hermitian case. While when $\gamma_d \neq 0$, a ring of EPs appears at $|\mathbf{k}| = k_c$, as observed in Figs. 1(a) and 1(b). We note that here ω_I is not purely dispersion-less for $|\mathbf{k}|$ far away from the ring of EPs, because the effective Hamiltonian is only an approximation near the frequency of the Dirac point ω_D [17].

From the aspect of the effective medium model with parameters and dispersion described by Eqs. (2) and (3), the solution of dispersion-less ω_R within the ring of EPs is $\omega_{\varepsilon_R} = \omega_{\mu_R} = \omega_D$. Therefore, we immediately have $\varepsilon_R = \mu_R = 0$ when $\omega_R = \omega_D$. At the Brillouin zone center (i.e. $|\mathbf{k}| = 0$) within the ring of EPs, we can obtain two solutions of Eq. (3), i.e., $\omega_I = \omega_{\varepsilon_I}$ (upper frequency) and $\omega_I = \omega_{\mu_I}$ (lower frequency), which correspond to $\varepsilon_I = 0$ and $\mu_I = 0$, respectively. The ring of EPs can be obtained at the frequency of (see Supplement 1 for detailed derivation),

$$\omega_R = \omega_D \text{ and } \omega_I = \frac{\omega_{\varepsilon_I} + \omega_{\mu_I}}{2} \tag{5}$$

with a radius of (in the **k** space)

$$k_{\mathrm{EP}} = \sqrt{A_\varepsilon A_\mu}\frac{\omega_D}{c}\frac{\omega_{\varepsilon_I} - \omega_{\mu_I}}{2}. \tag{6}$$

At the ring of EPs, the $\varepsilon(\omega_R, \omega_I)$ and $\mu(\omega_R, \omega_I)$ are purely imaginary, but with opposite signs. This result is consistent with previous effective medium studies of similar systems [23,24]. We note that the signs of the imaginary parts of $\varepsilon(\omega_R, \omega_I)$ and $\mu(\omega_R, \omega_I)$ are defined under ω_I<0. Therefore, they do not indicate the real gain or loss, but an "effective gain" or "effective loss" relative to the decaying behavior defined by ω_I<0 [26,27].

We further verify the effective medium parameters based on the eigenmode analysis [28,29]. Based on the band structures and the wave impedance regarding to eigenmodes, we obtain the complex effective parameters $\varepsilon(\omega)$ and $\mu(\omega)$ with respect to complex eigen-frequency ω (see details in Supplement 1). We find that nearby the Brillouin zone center ε_R and μ_R vary almost linearly with ω_R, while ε_I and μ_I vary almost linearly with ω_I, which is in accordance with Eq. (2). Through fitting the linear relations, the relevant parameters in Eq. (2) are retrieved as $A_{\varepsilon_R} = 3.645(a/2\pi c)$, $A_{\mu_R} = 10.749(a/2\pi c)$, $A_{\varepsilon_I} = 3.686(a/2\pi c)$, $A_{\mu_I} = 10.653(a/2\pi c)$, $\omega_{\varepsilon_R} \approx \omega_{\mu_R} \approx \omega_D = 0.541(2\pi c/a)$, $\omega_{\varepsilon_I} = -0.00447(2\pi c/a)$, $\omega_{\mu_I} = -0.0098(2\pi c/a)$. The corresponding effective permittivity and permeability are plotted in Figs. 1(c) and 1(d) as functions of ω_R and ω_I, respectively. It is observed in Figs. 1(c) and 1(d) that $\varepsilon_R = \mu_R = 0$ at $\omega_R = \omega_{\varepsilon_R} = \omega_{\mu_R} = \omega_D$, while $\varepsilon_I = 0$ at $\omega_I = \omega_{\varepsilon_I}$ and $\mu_I = 0$ at $\omega_I = \omega_{\mu_I}$. This result is consistent with the analysis by using the effective medium picture based on Eqs. (2) and (3). Moreover, we can see that $\mu_R = \mu_I = 0$ at $\omega_R = \omega_D$ and $\omega_I = \omega_{\mu_I}$. This perfectly explains the occurrence and position of additional flat band of longitudinal modes that emerges at $\omega_R = \omega_D$ and $\omega_I = \omega_{\mu_I}$ in the ω_R and ω_I band structures. Here, we note that the condition of $\varepsilon_R = \varepsilon_I = 0$ cannot induce flat bands of longitudinal modes because here we consider the TM polarization where the electric field is in the out-of-plane direction and cannot be longitudinal with the in-plane wave vector.

Optics EXPRESS

It is convenient to reconstruct the complex band structure by using Eq. (3) with the fitted parameters. Figures 1(e) and 1(f) show the retrieved ω_R and ω_I, respectively. The flat bands are plotted as horizontal gray lines according to the condition of $\mu_R = \mu_I = 0$. Clearly, the reconstructed band structures match well with those of the PhC obtained by finite-element numerical calculations (Figs. 1(a) and 1(b)). Note that the slight difference between the simulation results (Figs. 1(a) and 1(b)) and effective medium prediction (Figs. 1(e) and 1(f)) is caused by the linear approximation in the effective medium description. The dispersion-less ω_R within the ring of EPs, the shape of the ring, as well as the additional flat bands are all well predicted by the non-Hermitian effective medium theory. In the Supplement 1, we also show that the non-Hermitian effective medium gradually converges to the previous Hermitian one when the loss/gain in the system is reduced to zero.

Interestingly, we find that the radius of the exceptional ring can be manipulated and even shrinks into a point by simply engineering the loss/gain in the different components of the non-Hermitian PhC, as indicated by Eq. (6). In this case, the parameters of effective media have $\omega_{\varepsilon_R} = \omega_{\mu_R} = \omega_D$ and $\omega_{\varepsilon_I} = \omega_{\mu_I} = \omega_{DI}$. This indicates that Dirac-like cones are formed in both ω_R and ω_I band structures. In other words, the Dirac-like cone is formed in a complex frequency space of $\omega = \omega_R + i\omega_I$, rather than only in the real frequency space. Through some derivation, we obtain dispersions $\omega_R = \omega_D \pm \frac{\beta}{\omega_D}k$ and $\omega_I = \omega_{DI} \pm \frac{\beta\omega_{DI}}{{\omega_D}^2}k$ near the complex Dirac-like point (ω_D, ω_{DI}), where $\beta = c/\sqrt{A_\varepsilon A_\mu}$. This Dirac-cone like phenomenon in both real and imaginary frequency domain is absent in Hermitian systems like loss-less PhCs.

We note that this amazing phenomenon can be achieved in fully passive PhCs. For demonstration, we take the PhC model in Fig. 1 as an example, but the relative permittivities of the cylindrical rods and the background medium are changed to $\varepsilon_A = 12.5 + 0.33i$ and $\varepsilon_B = 1 + 0.0264i$, respectively. Here, we find that through varying the imaginary parts of ε_A and ε_B, the zero-crossing positions of effective ε_I and μ_I can be efficiently tuned, i.e., ω_{ε_I} and ω_{μ_I} are changed. While the slope of ε_I and μ_I with respect to ω_I remains unchanged, i.e., A_{ε_I} and A_{μ_I} remain unchanged (see Supplement 1). Therefore, here we can only engineer the imaginary parts of ε_A and ε_B to realize the condition $\omega_{\varepsilon_I} = \omega_{\mu_I} = \omega_{DI}$.

The corresponding complex band structures are calculated using software COMSOL Multiphysics, as plotted in Figs. 2(a) and 2(b). Interestingly, the ring of EPs disappears and a Dirac cone occurs in both the ω_R and ω_I band structures (more specifically, $\omega_R a/2\pi c = \omega_D a/2\pi c = 0.541$ in the ω_R spectrum, and $\omega_I a/2\pi c = -0.00714$ in the ω_I spectrum). The effective parameters of this PhC are retrieved and found to have linear dispersions satisfying Eq. (2) as the previous case. The relevant parameters are $A_{\varepsilon_R} \approx A_{\varepsilon_I} = 3.645(a/2\pi c)$,$A_{\mu_R} \approx A_{\mu_I} = 10.6(a/2\pi c)$, $\omega_{\varepsilon_R} \approx \omega_{\mu_R} = \omega_D = 0.541(2\pi c/a)$ and $\omega_{\varepsilon_I} \approx \omega_{\mu_I} = \omega_{DI} = -0.00714(2\pi c/a)$, respectively. The real and imaginary parts of ε and μ are plotted in Figs. 2(c) and 2(d), respectively. It is seen that $\varepsilon_R = \mu_R = 0$ at $\omega_R = \omega_D$, and $\varepsilon_I = \mu_I = 0$ at $\omega_I = \omega_{DI}$. The retrieved complex band structures based on these effective parameters (Figs. 2(e) and 2(f)) match well with the simulation results (Figs. 2(a) and 2(b)), confirming the validity of the effective medium picture. The additional flat band of longitudinal modes now crosses the complex Dirac point (ω_D, ω_{DI}) in the ω_R and ω_I band structures, because $\mu_R = \mu_I = 0$ at the complex Dirac point. This finding shows that the spawning ring of EPs can shrink to a complex Dirac point in a complex Dirac-like cone in a fully passive PhC.

Besides the case of $\omega_{\varepsilon_R} = \omega_{\mu_R} = \omega_D$ and $\omega_{\varepsilon_I} \neq \omega_{\mu_I}$ (ring of EPs) and the case of $\omega_{\varepsilon_R} = \omega_{\mu_R} = \omega_D$ and $\omega_{\varepsilon_I} = \omega_{\mu_I} = \omega_{DI} \neq 0$ (complex Dirac-like cones) discussed above, the non-Hermitian PhC can also possess effective parameters satisfying $\omega_{\varepsilon_R} \neq \omega_{\mu_R}$ and $\omega_{\varepsilon_I} = \omega_{\mu_I} = \omega_{DI}$. In this case, the Dirac-like cone in the ω_R band structure would split into a band gap, while the Dirac-like point in the ω_I band structure would be transformed into a point of quadratic degeneracy [30]. Through some derivation, we obtain dispersions $\omega_R = \omega_{\varepsilon_R} + \frac{\alpha}{{\omega_{\varepsilon_R}}^2(\omega_{\varepsilon_R} - \omega_{\mu_R})}k^2$, $\omega_R = \omega_{\mu_R} - \frac{\alpha}{{\omega_{\mu_R}}^2(\omega_{\varepsilon_R} - \omega_{\mu_R})}k^2$

Optics EXPRESS

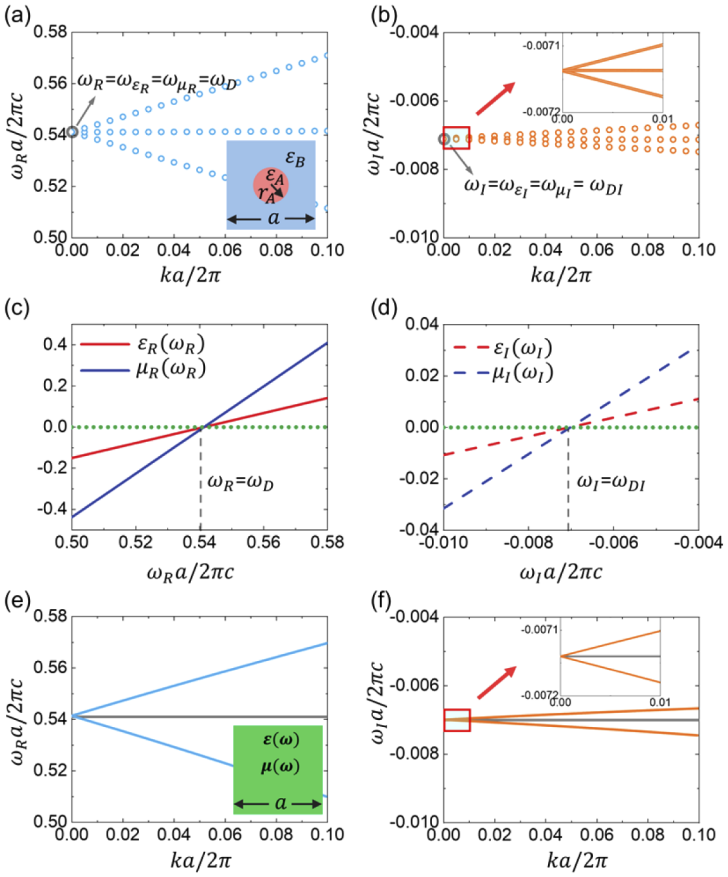

Fig. 2. [(a) and (b)] Complex band structures of a PhC composed of cylindrical rod with $\varepsilon_A = 12.5 + 0.33i$ in a background medium of $\varepsilon_B = 1 + 0.0264i$. (a) and (b), respectively, show the real and imaginary parts of eigen-frequencies for given real Bloch wave vectors based on numerical calculations. (c) Real and (d) imaginary parts of the effective parameters of this PhC. Retrieved (e) real and (f) imaginary parts of eigen-frequencies based on the effective parameters. The gray solid line denotes the longitudinal mode.

Optics EXPRESS

in the ω_R spectrum, and $\omega_I = \omega_{DI} - \frac{2\alpha\omega_{DI}}{\omega_{\varepsilon_R}{}^3(\omega_{\varepsilon_R}-\omega_{\mu_R})}k^2$, $\omega_I = \omega_{DI} + \frac{2\alpha\omega_{DI}}{\omega_{\mu_R}{}^3(\omega_{\varepsilon_R}-\omega_{\mu_R})}k^2$ in the ω_I spectrum, which indicates a point of quadratic degeneracy. Here $\alpha = c^2/A_\varepsilon A_\mu$.

As an example, we change the relative permittivities of PhC model studied in Fig. 1 to $\varepsilon_A = 12 + 0.33i$ and $\varepsilon_B = 1.04 + 0.02978i$. The corresponding complex band structures are plotted in Figs. 3(a) and 3(b). Evidently, a band gap appears in the ω_R band structure (Fig. 3(a)), while a point of quadratic degeneracy is seen in the ω_I band structure (Fig. 3(b)). The effective parameters are retrieved and found to have linear dispersions. The relevant parameters are obtained as $A_{\varepsilon_R} \approx A_{\varepsilon_I} = 3.804(a/2\pi c)$, $A_{\mu_R} \approx A_{\mu_I} = 10.380(a/2\pi c)$, $\omega_{\varepsilon_R} = 0.539(2\pi c/a)$, $\omega_{\mu_R} = 0.550(2\pi c/a)$ and $\omega_{\varepsilon_I} \approx \omega_{\mu_I} = \omega_{DI} = -0.00759(2\pi c/a)$. The real and imaginary parts of ε and μ are presented in Figs. 3(c) and 3(d), respectively. The retrieved complex band structure by using these effective parameters are presented in Figs. 3(e) and 3(f), which match well with the simulation results (Figs. 3(a) and 3(b)). The band edges in the ω_R band structure are determined by $\omega_R = \omega_{\varepsilon_R}$ and $\omega_R = \omega_{\mu_R}$. The additional flat band of longitudinal modes is induced by $\mu_R = \mu_I = 0$ at the frequency of $\omega_R = \omega_{\mu_R}$ and $\omega_I = \omega_{\mu_I} = \omega_{\varepsilon_I}$. This finding shows that quadratic degeneracy can be realized in the ω_I band structure by simply designing $\omega_{\varepsilon_I} = \omega_{\mu_I} = \omega_{DI}$.

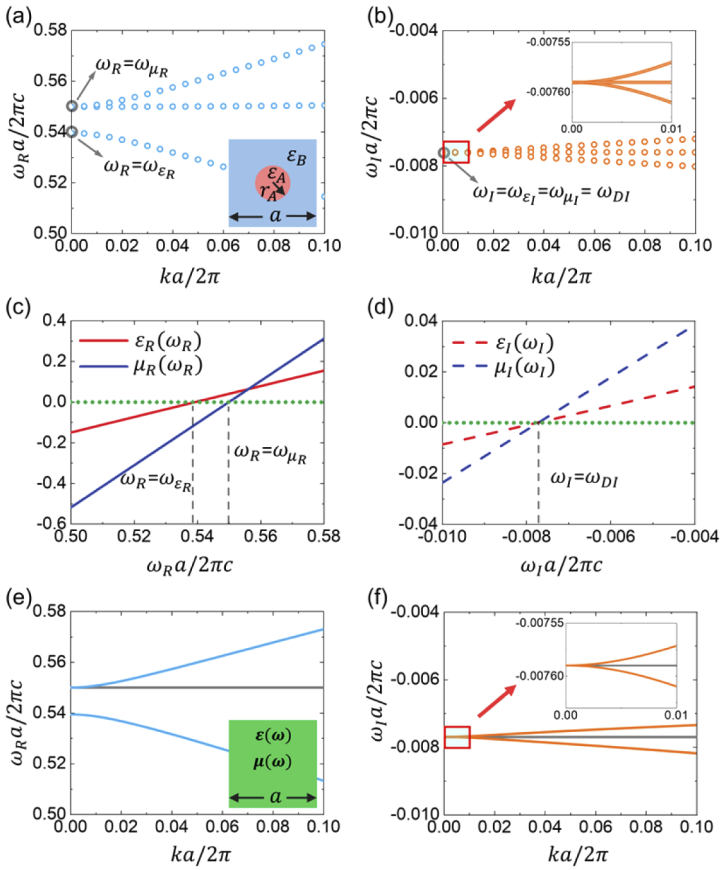

Fig. 3. [(a) and (b)] Complex band structures of a PhC composed of cylindrical rod with $\varepsilon_A = 12 + 0.33i$ in background medium of $\varepsilon_B = 1.04 + 0.02978i$. (a) and (b), respectively, show the real and imaginary parts of eigen-frequencies for given real Bloch wave vectors based on numerical calculations. (c) Real and (d) imaginary parts of the effective parameters of this PhC. Retrieved (e) real and (f) imaginary parts of eigen-frequencies based on the effective parameters. The gray solid line denotes the longitudinal mode.

Optics EXPRESS

Table 1 summarizes the features of band structures for different types of parameters discussed in Figs. 1–3 based on the non-Hermitian medium description. Interesting characteristics of complex band structures including the ring of EPs, complex Dirac-like cones, quadratic degeneracy and flat bands of longitudinal modes are observed by simply adjusting the loss in the PhC. We note that the many of the predicted phenomena are clearly beyond the description of the Hamiltonian model for the ring of EPs. The non-Hermitian effective medium theory, however, can interpret all the above phenomena and is thus universal.

Table 1. Features of band structures of non-Hermitian PhCs with loss

	Characteristics of parameters		Features of band structures		Flat band
	$\omega_{\varepsilon_R},\ \omega_{\mu_R}$	$\omega_{\varepsilon_I},\ \omega_{\mu_I}$	Real parts	Imaginary parts	
Case 1 (Fig. 1)	$\omega_{\varepsilon_R}=\omega_{\mu_R}=\omega_D$	$\omega_{\varepsilon_I}\neq\omega_{\mu_I}$	Dispersion-less within EP ring	Ring of EPs	@ $\omega_R=\omega_D$, $\omega_I=\omega_{\mu_I}$
Case 2 (Fig. 2)	$\omega_{\varepsilon_R}=\omega_{\mu_R}=\omega_D$	$\omega_{\varepsilon_I}=\omega_{\mu_I}=\omega_{DI}$	Dirac-like cone	Dirac-like cone	@ $\omega_R=\omega_D$, $\omega_I=\omega_{DI}$
Case 3 (Fig. 3)	$\omega_{\varepsilon_R}\neq\omega_{\mu_R}$	$\omega_{\varepsilon_I}=\omega_{\mu_I}=\omega_{DI}$	Band gap	Quadratic degeneracy	@ $\omega_R=\omega_{\mu_R}$, $\omega_I=\omega_{DI}$

The above discussions are within the picture of complex eigen-frequencies and real Bloch wave vectors. In fact, we have also investigated the validity of the non-Hermitian effective medium theory under the other picture of real eigen-frequencies and complex Bloch wave vectors. The results also prove the validity of the non-Hermitian effective medium theory, and the details are presented in the Supplement 1.

In summary, we have proposed a local non-Hermitian effective medium theory that can accurately predict the spawning ring of exceptional points in photonic crystals with loss/gain. Based on this theory, we also predict the existence of complex Dirac-like cones with Dirac conical dispersions, the quadratic degeneracy and the additional flat bands in the band structures of real and imaginary frequencies. By engineering non-Hermitian photonic crystals, we have numerically realized such effective media with complex Dirac-like cones or quadratic degeneracy. Our work thus opens a gate for exploring the rich physics in non-Hermitian effective media.

Funding. National Key Research and Development Program of China (2020YFA0211300, 2017YFA0303702); National Natural Science Foundation of China (11974176, 61671314); Priority Academic Program Development of Jiangsu Higher Education Institutions.

Disclosures. The authors declare no conflicts of interest.

Data availability. Data underlying the results presented in this paper are not publicly available at this time but may be obtained from the authors upon reasonable request.

Supplemental document. See Supplement 1 for supporting content.

References

1. V. A. Markel, "Introduction to the Maxwell Garnett approximation: tutorial," J. Opt. Soc. Am. A **33**(7), 1244 (2016).
2. C. R. Simovski, "On electromagnetic characterization and homogenization of nanostructured metamaterials," J. Opt. **13**(1), 013001 (2011).
3. T. J. Cui, W. X. Tang, X. M. Yang, Z. L. Mei, and W. X. Jiang, *Metamaterials: Beyond Crystals, Noncrystals, and Quasicrystals*. (CRC, 2016).
4. J. D. Joannopoulos, S. G. Johnson, J. N. Winn, and R. D. Meade, *Photonic Crystals: Molding the Flow of Light*, 2 Ed. (Princeton University, Princeton, USA, 2008).
5. X. Huang, Y. Lai, Z. H. Hang, H. Zheng, and C. T. Chan, "Dirac cones induced by accidental degeneracy in photonic crystals and zero-refractive-index materials," Nat. Mater. **10**(8), 582–586 (2011).
6. P. Moitra, Y. Yang, Z. Anderson, I. I. Kravchenko, D. P. Briggs, and J. Valentine, "Realization of an all-dielectric zero-index optical metamaterial," Nat. Photonics **7**(10), 791–795 (2013).

Optics EXPRESS

7. J. Dong, M. Chang, X. Huang, Z. H. Hang, Z. Zhong, W. Chen, Z. Huang, and C. T. Chan, "Conical dispersion and effective zero refractive index in photonic quasicrystals," Phys. Rev. Lett. **114**(16), 163901 (2015).
8. Y. Li, S. Kita, P. Muñoz, O. Reshef, D. I. Vulis, M. Yin, M. Lončar, and E. Mazur, "On-chip zero-index metamaterials," Nat. Photonics **9**(11), 738–742 (2015).
9. S. Kita, Y. Li, P. Camayd-Muñoz, O. Reshef, D. I. Vulis, R. W. Day, E. Mazur, and M. Lončar, "On-chip all-dielectric fabrication-tolerant zero-index metamaterials," Opt. Express **25**(7), 8326 (2017).
10. T. Dong, J. Liang, S. Camayd-Muñoz, Y. Liu, H. Tang, S. Kita, P. Chen, X. Wu, W. Chu, E. Mazur, and Y. Li, "Ultra-low-loss on-chip zero-index materials," Light: Sci. Appl. **10**(1), 10 (2021).
11. H. Chu, Q. Li, B. Liu, J. Luo, S. Sun, Z. H. Hang, L. Zhou, and Y. Lai, "A hybrid invisibility cloak based on integration of transparent metasurfaces and zero-index materials," Light: Sci. Appl. **7**(1), 50 (2018).
12. J. Luo, B. Liu, Z. H. Hang, and Y. Lai, "Coherent perfect absorption via photonic doping of zero-index media," Laser Photonics Rev. **12**(8), 1800001 (2018).
13. D. Wang, J. Luo, Z. Sun, and Y. Lai, "Transforming zero-index media into geometry-invariant coherent perfect absorbers via embedded conductive films," Opt. Express **29**(4), 5247 (2021).
14. M. Dubois, C. Shi, X. Zhu, Y. Wang, and X. Zhang, "Observation of acoustic Dirac-like cone and double zero refractive index," Nat. Commun. **8**(1), 14871 (2017).
15. M. Minkov, I. A. D. Williamson, M. Xiao, and S. Fan, "Zero-index bound states in the continuum," Phys. Rev. Lett. **121**(26), 263901 (2018).
16. C. Xu, G. Ma, Z. Chen, J. Luo, J. Shi, Y. Lai, and Y. Wu, "Three-dimensional acoustic double-zero-index medium with a fourfold degenerate Dirac-like point," Phys. Rev. Lett. **124**(7), 074501 (2020).
17. B. Zhen, C. W. Hsu, Y. Igarashi, L. Lu, I. Kaminer, A. Pick, S. Chua, J. D. Joannopoulos, and M. Soljačić, "Spawning rings of exceptional points out of Dirac cones," Nature **525**(7569), 354–358 (2015).
18. P. M. Kamiński, A. Taghizadeh, O. Breinbjerg, J. Mørk, and S. Arslanagić, "Control of exceptional points in photonic crystal slabs," Opt. Lett. **42**(15), 2866 (2017).
19. D. I. Vulis, Y. Li, O. Reshef, P. Camayd-Muñoz, M. Yin, S. Kita, M. Lončar, and E. Mazur, "Monolithic CMOS-compatible zero-index metamaterials," Opt. Express **25**(11), 12381–12399 (2017).
20. Q. Wang, K. Ding, H. Liu, S. Zhu, and C. T. Chan, "Exceptional cones in 4D parameter space," Opt. Express **28**(2), 1758 (2020).
21. H. Xue, Q. Wang, B. Zhang, and Y. D. Chong, "Non-Hermitian Dirac cones," Phys. Rev. Lett. **124**(23), 236403 (2020).
22. N. Wang, R. Zhang, C. T. Chan, and G. P. Wang, "Effective medium theory for a photonic pseudospin-1/2 system," Phys. Rev. B **102**(9), 094312 (2020).
23. X. Cui, K. Ding, J. Dong, and C. T. Chan, "Realization of complex conjugate media using non-PT-symmetric photonic crystals," Nanophotonics **9**(1), 195–203 (2019).
24. X. Cui, K. Ding, J. Dong, and C. T. Chan, "Exceptional points and their coalescence of PT-symmetric interface states in photonic crystals," Phys. Rev. B **100**(11), 115412 (2019).
25. D. G. Baranov, A. Krasnok, and A. Alù, "Coherent virtual absorption based on complex zero excitation for ideal light capturing," Optica **4**(12), 1457 (2017).
26. H. Li, A. Mekawy, A. Krasnok, and A. Alù, "Virtual parity-time symmetry," Phys. Rev. Lett. **124**(19), 193901 (2020).
27. Y. Sun, W. Tan, H. Li, J. Li, and H. Chen, "Experimental demonstration of a coherent perfect absorber with PT phase transition," Phys. Rev. Lett. **112**(14), 143903 (2014).
28. J. Luo, Y. Yang, Z. Yao, W. Lu, B. Hou, Z. H. Hang, C. T. Chan, and Y. Lai, "Ultratransparent media and transformation optics with shifted spatial dispersions," Phys. Rev. Lett. **117**(22), 223901 (2016).
29. S. Li, Y. Wang, W. Zhang, W. Lu, B. Hou, J. Luo, and Y. Lai, "Observation of wide-angle impedance matching in terahertz photonic crystals," New J. Phys. **22**(2), 023033 (2020).
30. Y. D. Chong, X. Wen, and M. Soljačić, "Effective theory of quadratic degeneracies," Phys. Rev. B **77**(23), 235125 (2008).